AGU PUBLICATIONS

Earth's Future

Supporting Information for

Diagnosing phosphorus limitations in natural terrestrial ecosystems in carbon cycle models

Yan Sun[1,2], Shushi Peng[1*], Daniel S. Goll[2], Philippe Ciais[2], Bertrand Guenet[2], Matthieu Guimberteau[2,3], Philippe Hinsinger[4], Ivan A. Janssens[5], Josep Peñuelas[6,7], Shilong Piao[1,8], Benjamin Poulter[9], Aurélie Violette[2], Xiaojuan Yang[10], Yi Yin[2], Hui Zeng[11]

[1] Sino-French Institute for Earth System Science, College of Urban and Environmental Sciences, Peking University, Beijing 100871, China

[2] Laboratoire des Sciences du Climat et de 1'Environnement, CEA-CNRS-UVSQ, F-91191 Gif sur Yvette, France

[3] Sorbonne Universités, UPMC, CNRS, EPHE, UMR7619 METIS, 75252 Paris, France

[4] INRA, UMR Eco&Sols, Place Viala, 34060 Montpellier cedex, France

[5] Research Group of Plant and Vegetation Ecology (PLECO), Department of Biology, University of Antwerp, B-2610 Wilrijk, Belgium

[6] CSIC, Global Ecology Unit CREAF-CSIC-UAB, Cerdanyola del Vallès, 08193 Catalonia, Spain

[7] CREAF, Cerdanyola del Vallès, 08193 Catalonia, Spain

[8] Institute of Tibetan Plateau Research, Chinese Academy of Sciences, Beijing 100085, China

[9] Institute on Ecosystems and the Department of Ecology, Montana State University, Bozeman, MT 59717, USA

[10] Oak Ridge National Lab, Oak Ridge, TN 37831, USA

[11] Peking University Shenzhen Graduate School, Shenzhen 518055, China

Contents of this file

Text S1 to S2
Figures S1 to S14
Tables S1 to S5

Introduction

Test S1 describes the details of the soil type maps, soil C and P maps used in this study. Test S2 describes the methods for calculating soil organic P and soil organic C. Table S1 describes the basic information of three ESMs used in this study. Table S2 shows the results of P deficit derived from C stock approach and

NPP approach, respectively. Table S3 and S4 show the result of changes in reconstructed C stock and changes in reconstructed NPP due to P limitation, respectively. Table S5 show the additional P demand derived from C stock-based approach by using constant vegetation C:P ratios and flexible vegetation. Figure S1 shows additional P demand for changes in total terrestrial carbon stocks and each carbon pool under RCP2.6.Figure S2 presents changes of NPP, annual additional P demand and cumulative additional P demand under RCP2.6. Figure S3 shows spatial patterns of mean additional P demand by 2100 based on C stock approach, NPP_L1 and NPP_L2 approach under RCP2.6. Figure S4 and Figure S5 present the distributions of coefficient variation of additional P demand under RCP2.6 and RCP 8.5, respectively. Figure S6 shows spatial patterns of mean P deficit by 2100 based on C stock approach, NPP_L1 and NPP_L2 approach under RCP2.6. Figure S7 presents total cumulative soil P deficit by 2100 for 12 land regions as estimated by different scenarios of available soil P (S0-S3) under RCP2.6. Figure S8 shows the changes in percentages of pixels with soil P deficit in tropical regions. Figure S9 shows global P deficit by 2050 and 2100 derived from C stock approach, NPP_L1 and NPP_L2 approach. Figure S10 shows changes in compatible C stock and NPP by 2050 and 2100 considering P deficit. Figure S11 shows the C:P of SOM estimated based on Monte-Carlo method for each soil order. Figure S12 shows the changes in soil C stock and biomass. Figure S13 shows the utilization rates of resin Pi, labile Pi and labile P under RCP2.6 and RCP8.5 by 2100. Figure S14 shows the changes of annual additional P demand based on NPP approach derived from constant NPP allocations and modeled allocations by IPSL model. Figure S15 describes the changes of annual additional P demand based on NPP approach derived from the constant and time varying vegetation C:P ratios of leaf, wood and root.

Text S1.

Global soil order maps

Concentrations of different forms of soil P depend mainly upon parent material and stage of soil development in the absence of P fertilization (Vitousek et al., 2010; Yang & Post, 2011). To classify soils according to their weathering stage, we followed the classification applied by Yang et al. (2013) who combined two soil maps available in the SoilGrids1km product (http://soilgrids.org) (1) the USDA (United States Department of Agriculture) database for all regions except for Latin America and the (2) SOTERLAC soil order database for Latin America (Soil and Terrain database for Latin America and the Caribbean). This combined map was used to derive the global distribution of different forms of soil P. The USDA global gridded map of soil orders described by Hengl et al. (2014) was obtained by interpolation from 110,000 soil samples using geostatistical methods. This map with 1 km spatial resolution uses the USDA classification system including 58 soil suborders (ftp://ftp.soilgrids.org/data/archive/5.Dec.2013/). The SOTERLAC soil order map (version 2.0, http://www.isric.org/projects/soter-latin-america-and-caribbean-soterlac) was compiled using GIS and SOTER methodology (Dijkshoorn et al., 2005). We used the same combined USDA and SOTERLAC soil order maps as Yang et al. (2013) to ensure consistency between our estimates of P demand and soil P availability data published by Yang et al. (2013).

Soil phosphorus map and soil organic carbon (C) map

We used spatial information on soil P content from Yang et al. (2013) who derived global gridded estimates for 6 different forms of soil P: total, labile inorganic, organic, secondary mineral, occluded and apatite P, respectively, at a spatial resolution of 0.5 degree by using a compilation of measurements from the Hedley sequential fractionation methods (Hedley et al., 1982; Tiessen & Moir, 1993) combined with maps of parent bedrock material. The USDA soil organic C (SOC) map contains entries for 6 soil depths intervals (0~5, 5~15, 15~30, 30~60, and 60~120 cm) at 1 km resolution by interpolation methods (3D regression with splines; http://www.isric.org/content/faq-soilgrids).

Text S2.

Dealing with SOC from USDA and SOP from Yang et al. (2013)

Soil bulk density corresponding to each depth is used to convert SOC from g C /kg soil to g/m^2 as Eq. S1:

$$soc_m = \sum_{l=1}^{4} soc_{i,l} \times \rho_{bl} \times d_l \qquad \text{(Eq. S1)}$$

Where soc_m refers to soil organic C (g C / m^2 soil), $soc_{i,l}$ for soil organic C for soil layer l (g C / kg soil), ρ_{bl} for soil bulk density for soil layer l (kg /m3 soil), and d_l for thickness of the soil layer l (m).

Note that SOP was only provided in the top 50 cm soil by Yang et al. (2013). We thus used the C:P ratio of SOM in the top 50 cm soil to represent the C:P ratios of whole SOM pools. With the assumption of uniform vertical distribution of SOC in soil depth range of 30~60 cm, we summed SOC from USDA by 5 top depths ranges into SOC of 0~50 cm.

Data Availability

The source data used in this study can be available by the links in Data and Material and Text S1. The complete datasets of global gridded soil and vegetation C:P ratios can be requested from the corresponding author.

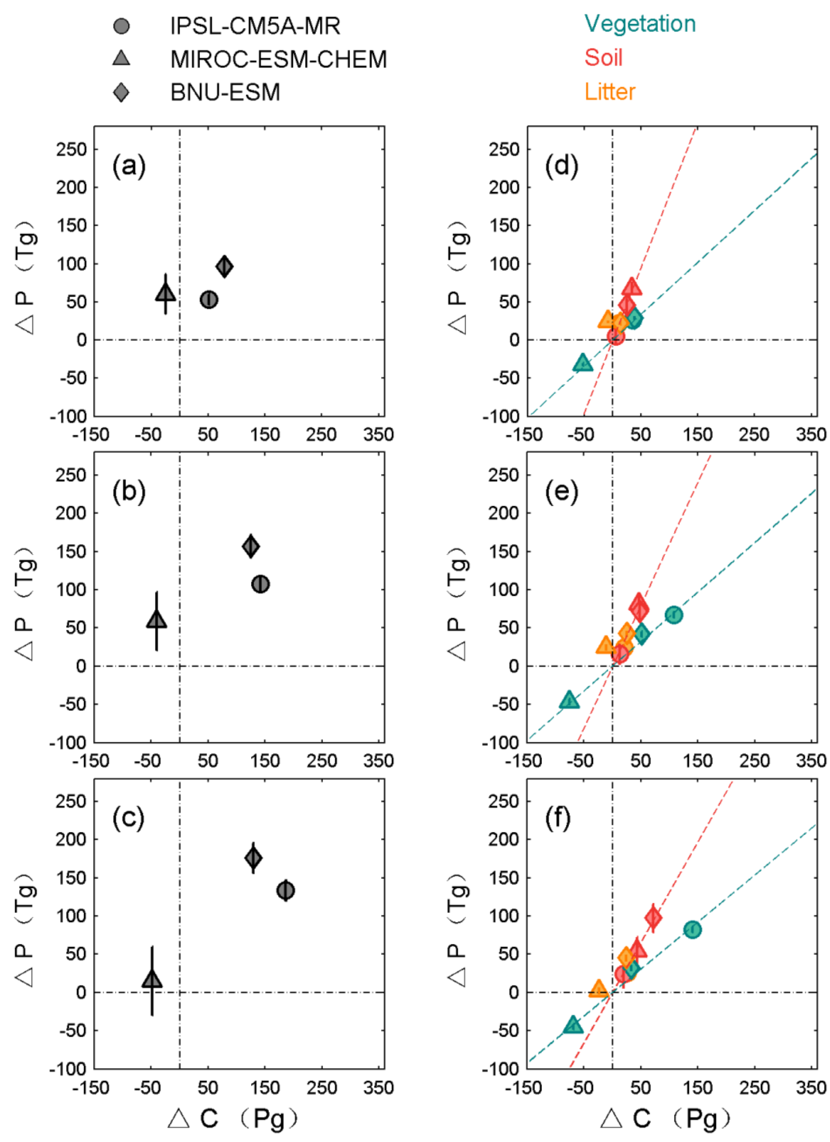

Figure S1 Additional P demand for changes in total terrestrial carbon stocks (a, b and c) and each carbon pool (d, e and f) under RCP2.6 estimated by the three CMIP5 models from 1900 to 2005 (a, d), 2050 (b, e) and 2100 (c, f), respectively. Changes of P demand for soil, vegetation and litter pools are discriminated by red, green and orange respectively. Error bars shown in total and soil P demand indicate the variations estimated by uncertain C:P ratios in soil organic matters, litter and plant tissues.

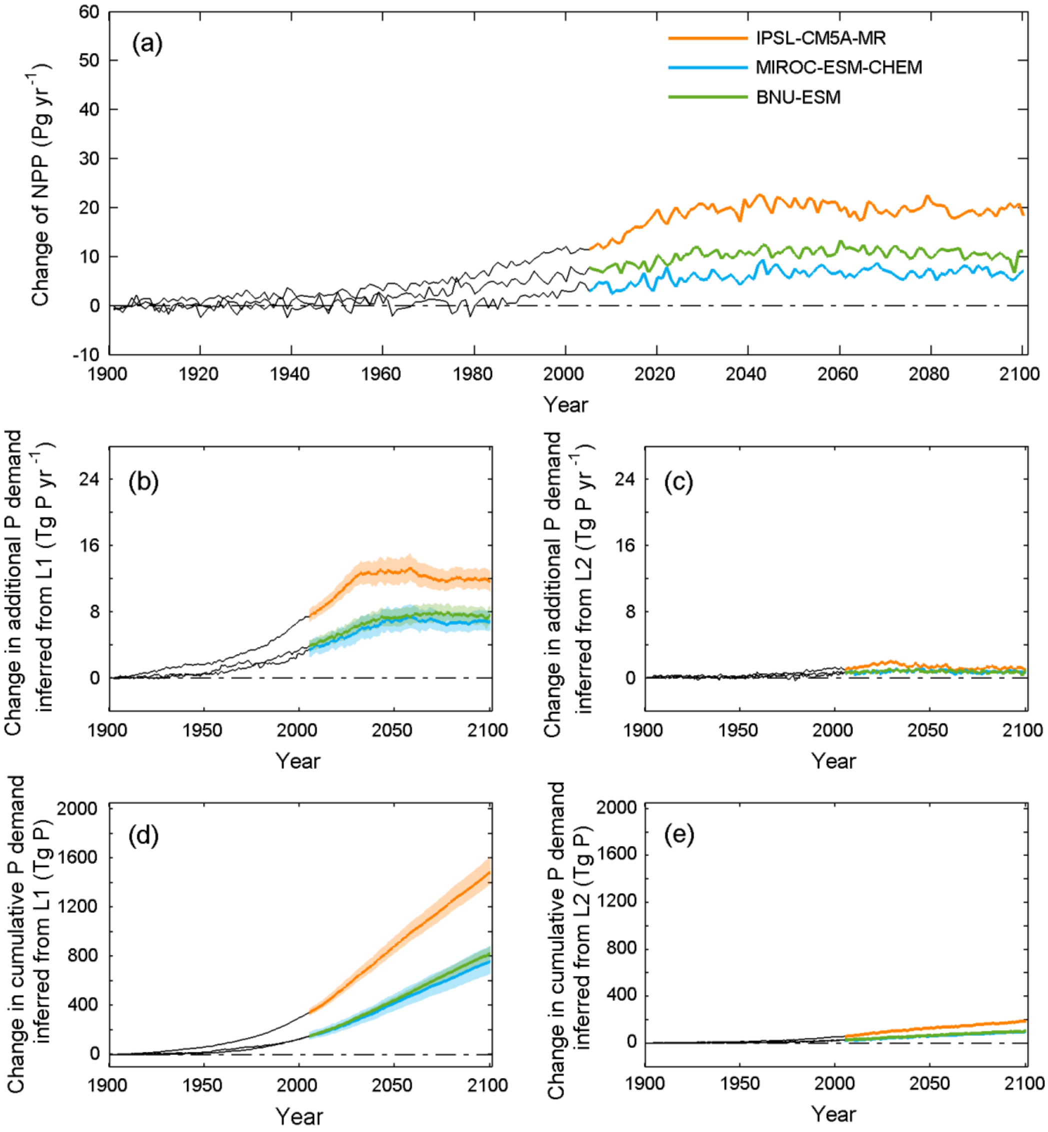

Figure S2 Changes of NPP (a), annual additional P demand (b for L1, c for L2; running average with 15-years window) and cumulative additional P demand (d for L1, e for L2) relative to 1900-1910 under RCP2.6 derived from three models. Shading indicates the variations of P demand (standard deviation) considering the uncertainty of plant tissue C:P ratios.

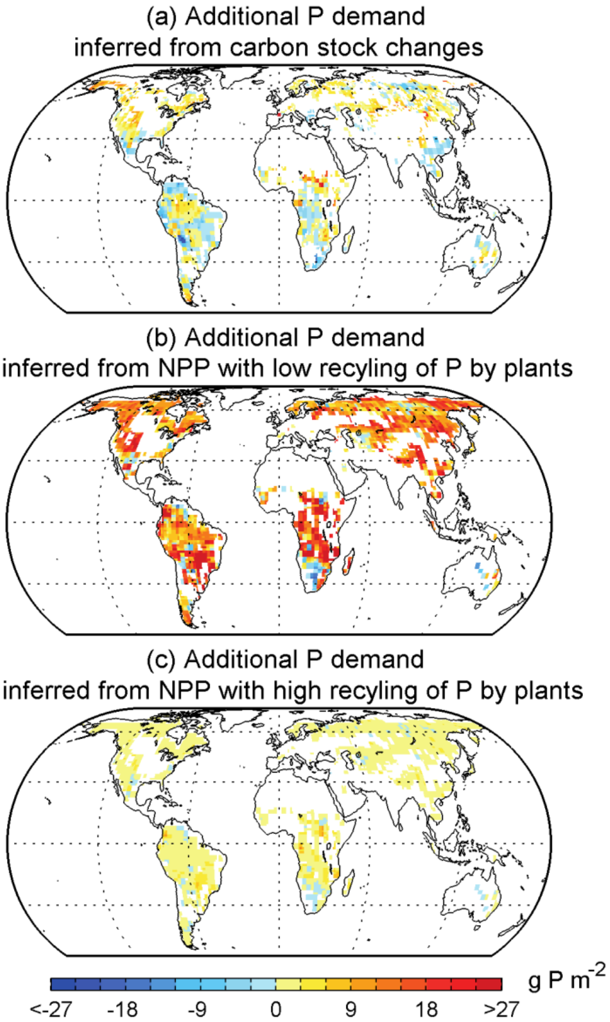

Figure S3 Spatial patterns of mean additional P demand across three models based on the changes of terrestrial pools (a) and NPP (b, c for L1; e, f for L2) from 1900 to 2100 for RCP2.6.

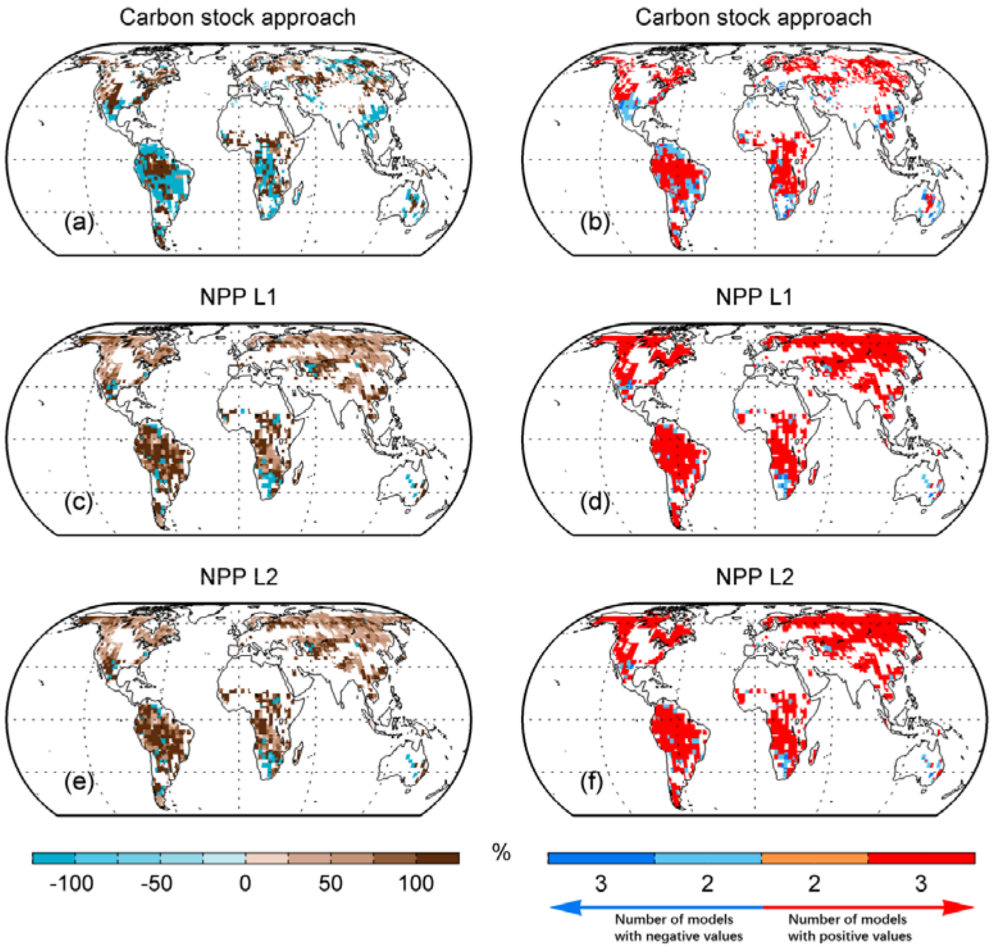

Figure S4 Distributions of coefficient variation (a, c, e) and number of model simulations with same direction of additional P demand (b, d, f) under RCP2.6.

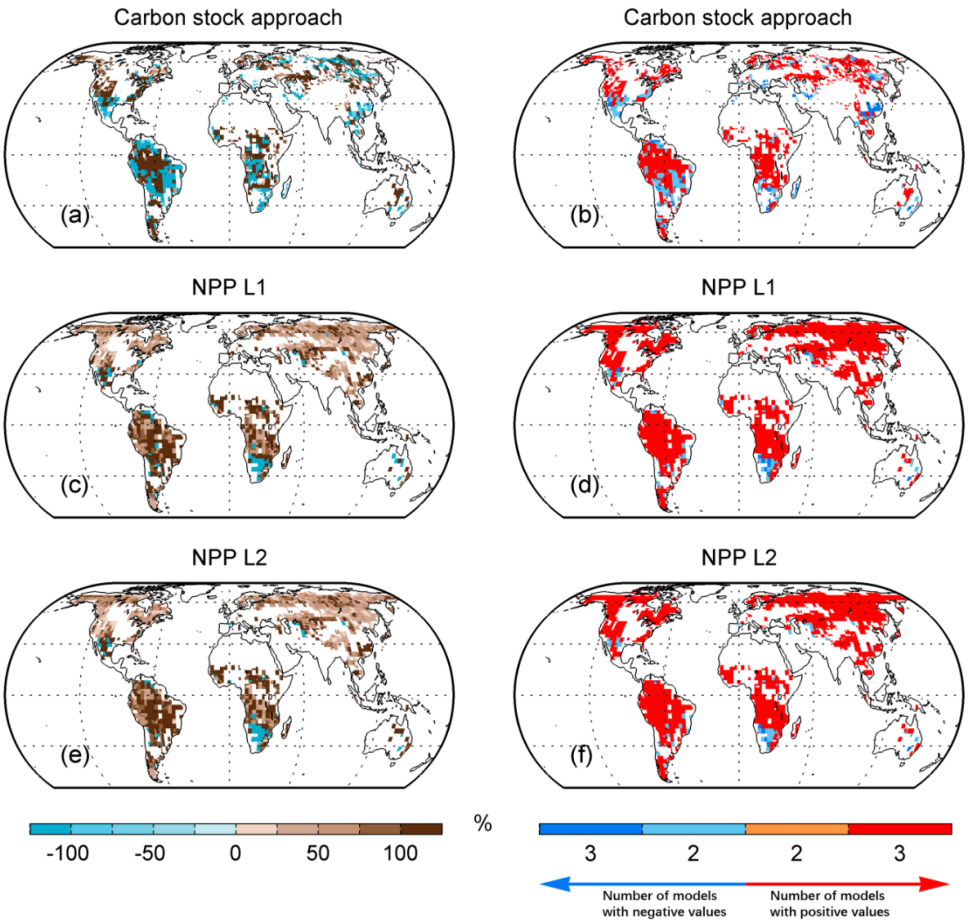

Figure S5 Distributions of coefficient variation (a, c, e) and number of model simulations with same direction of additional P demand (b, d, f) under RCP8.5.

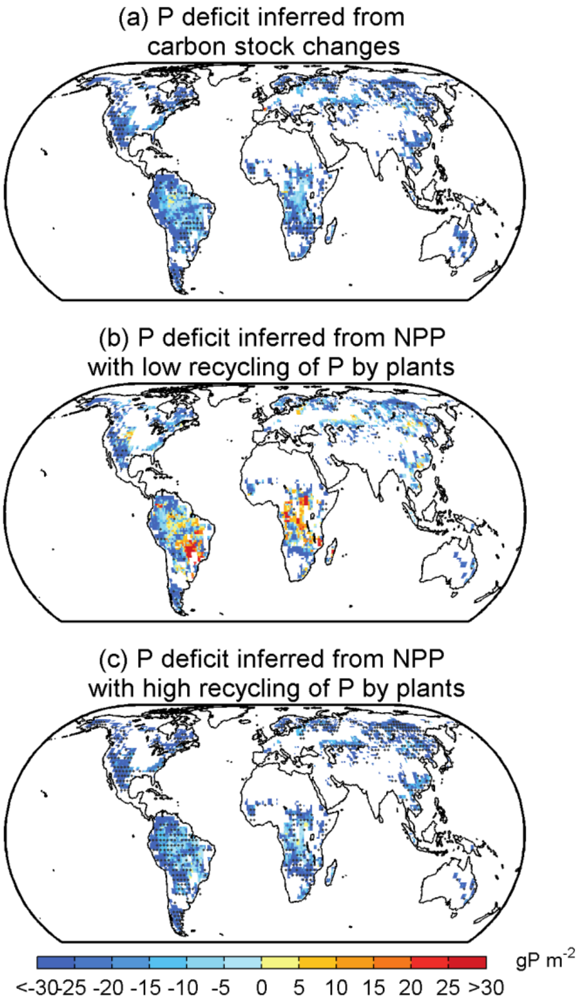

Figure S6 Spatial patterns of mean P deficit (g P m-2) across the three CMIP5 models by 2100 under RCP2.6 and the medium soil P availability (labile inorganic P) scenario. Negative P deficit indicates P demand is smaller than P supply. Note that negative P deficit is included in calculating mean P deficit, this figure only present the distribution of P deficit but cannot be used to infer the total P deficit. a) shows global patterns of P deficit derived from carbon pool, and b) and c) refer the results from the NPP-based approach with different litter mineralization scenarios (b for L1; c for L2) with black points indicating coefficient of variation (ratios of standard deviation and mean values of P deficit) < 25%.

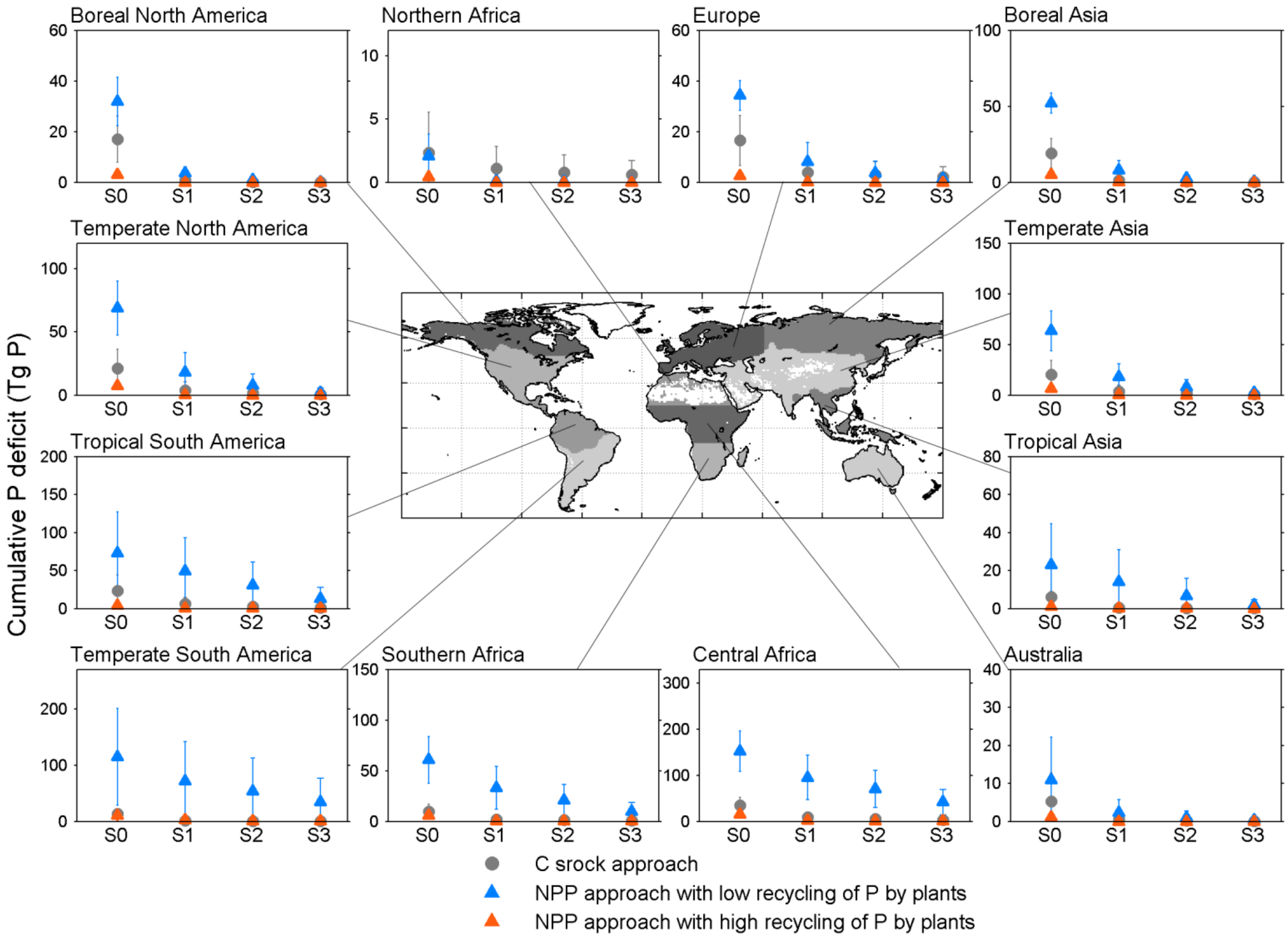

Figure S7 Scatter plots showing total cumulative soil P deficit (Tg P) by 2100 for 12 land regions as estimated by different scenarios of available soil P (S0-S3) under RCP2.6. Regional P deficit is given as the sum of P deficit from grids with positive deficit. Soil P deficit derived from carbon pool and two scenarios in the NPP-based approach (NPP_L1 and NPP_L2) are discriminated by grey, blue and orange respectively. Markers and error bars indicate the mean values and standard deviations among estimates from three ESMs and uncertain C:P ratios for plant tissues, litter and SOM. The divisions of land regions are shown in the map.

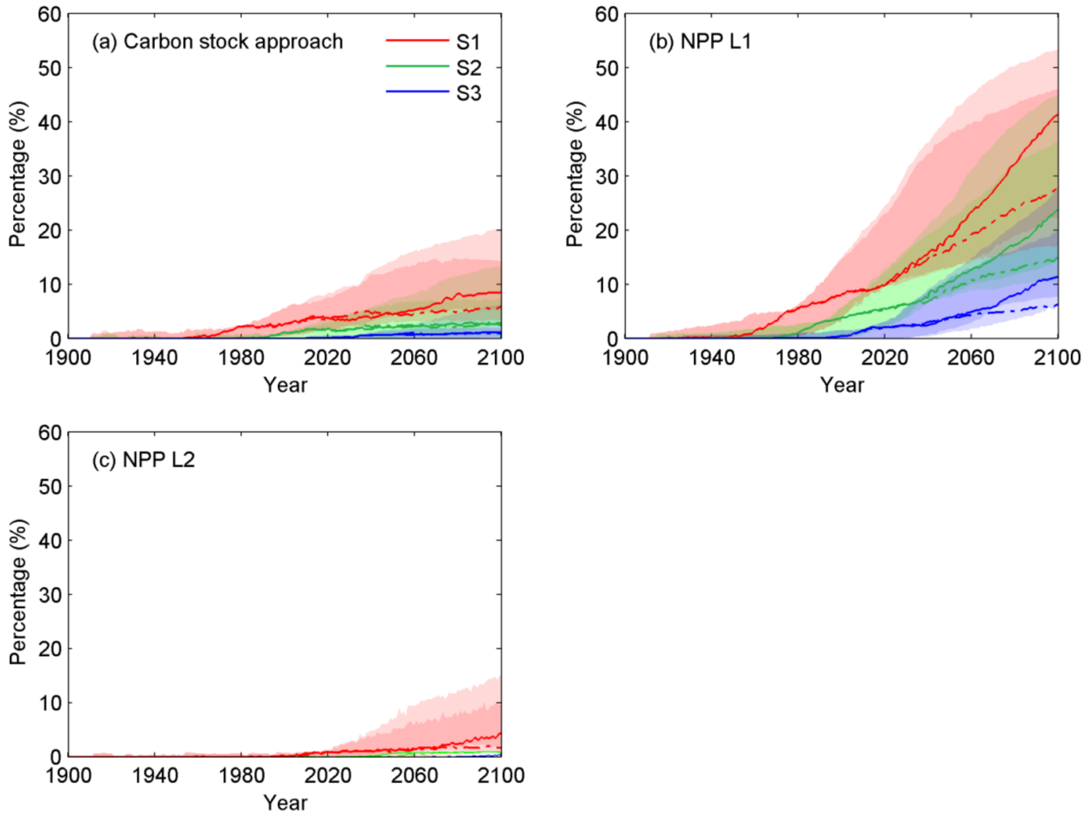

Figure S8 Changes in percentages of pixels with soil P deficit in tropical regions (including Central Asia, Tropical South America and Tropical Asia, of which divisions have been shown in figure 7) under three scenarios of soil P availability (S1 for resin inorganic P, S2 for labile inorganic P and S3 for labile inorganic and organic P). Dotted and solid lines represent RCP2.6 and RCP8.5 respectively. Shading indicates the variations of percentages by three models.

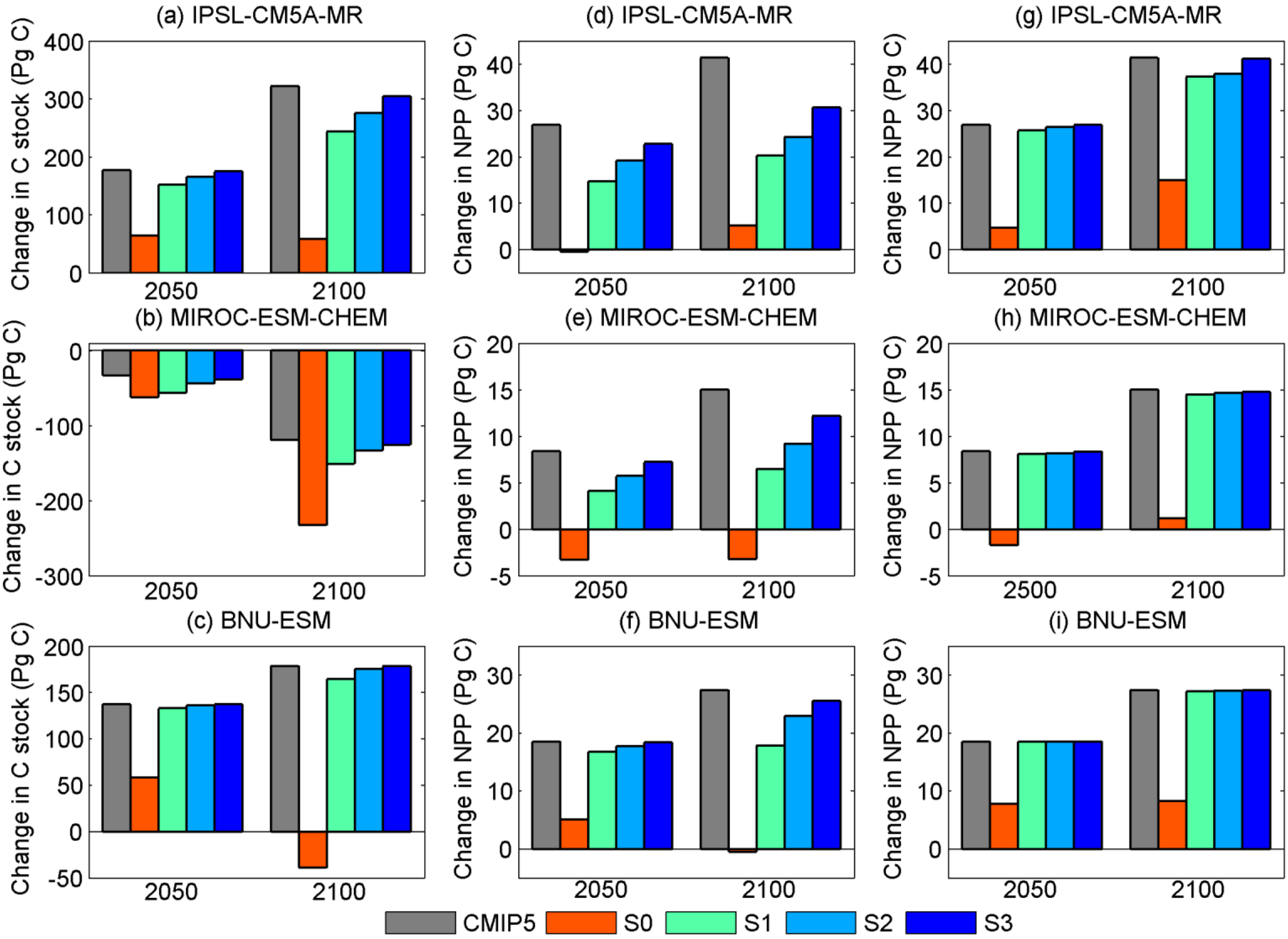

Figure S9 Changes in compatible C stock and NPP by 2050 and 2100 under RCP8.5. Panels in the first, second and third row indicate IPSL-CM5A-MR, MIROC-ESM-CHEM and BNU-ESM, respectively. (a)-(c) show the changes of realized C stock considering P deficit diagnosed from C stock approach. (d)-(f) refer the changes of realized NPP considering P deficit diagnosed from NPP_L1 approach. (g)-(i) show the changes of realized NPP considering P deficit diagnosed from NPP_L2 approach.

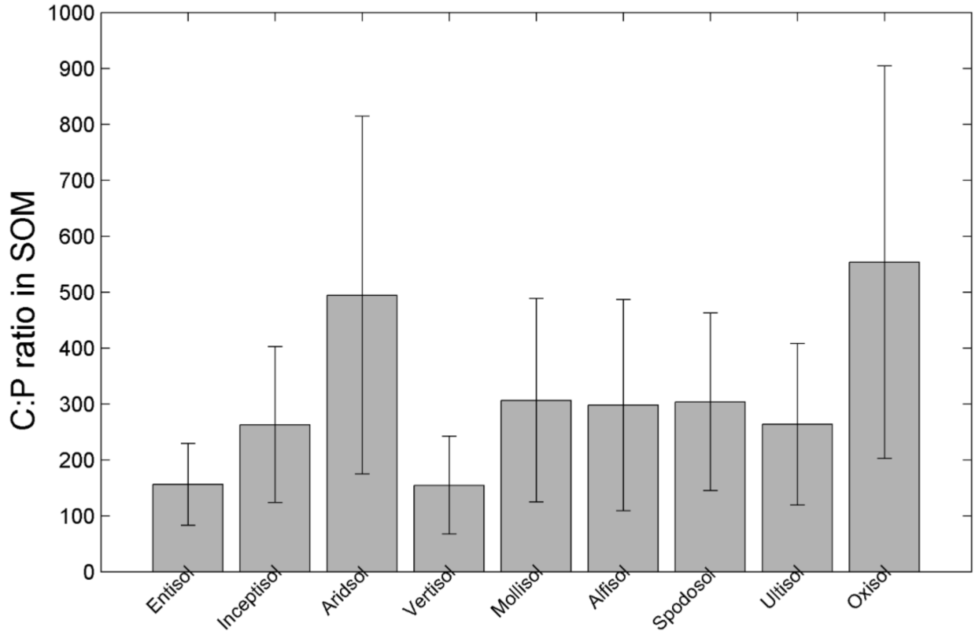

Figure S10 C:P of SOM estimated based on Monte-Carlo method for each soil order. Uncertainty of SOC stock is estimated by 10th and 90th quartiles in USDA. The uncertainty of SOC for each soil order is estimated as standard deviation with the assumption that SOC follows a logarithmic normal distribution. This uncertainty includes both biases of site-measurements that were used by the USDA dataset and on the spatial variance of SOC in that dataset. The uncertainty of organic P for each soil order is estimated by using quadratic propagation (Yang et al., 2013). 500 sets of suborder-specific C: P ratios of SOM are obtained by using a Monte-Carlo method. Bars and errors indicate the median and the median absolute deviations respectively.

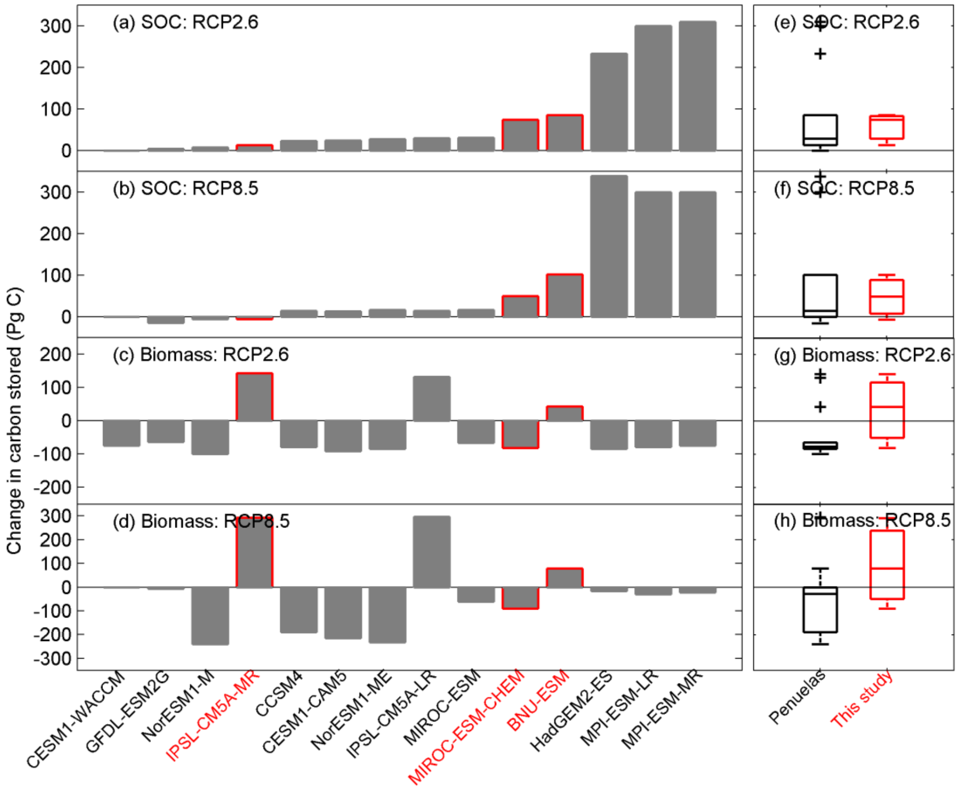

Figure S11 Changes in soil C stock (a, b) and biomass (c, d) derived from 14 ESMs used by Peñuelas et al (2013) (grey bars) and 3 models used in this study (grey bars with red edges). (a) and (c) refer to the RCP2.6, (b) and (d) for the RCP8.5. (e)-(h) show the Box-whisker plot of changes in SOC (e, f) and biomass (g, h) derived from 14 ESMs used by Peñuelas et al (2013) and 3 models used in this study.

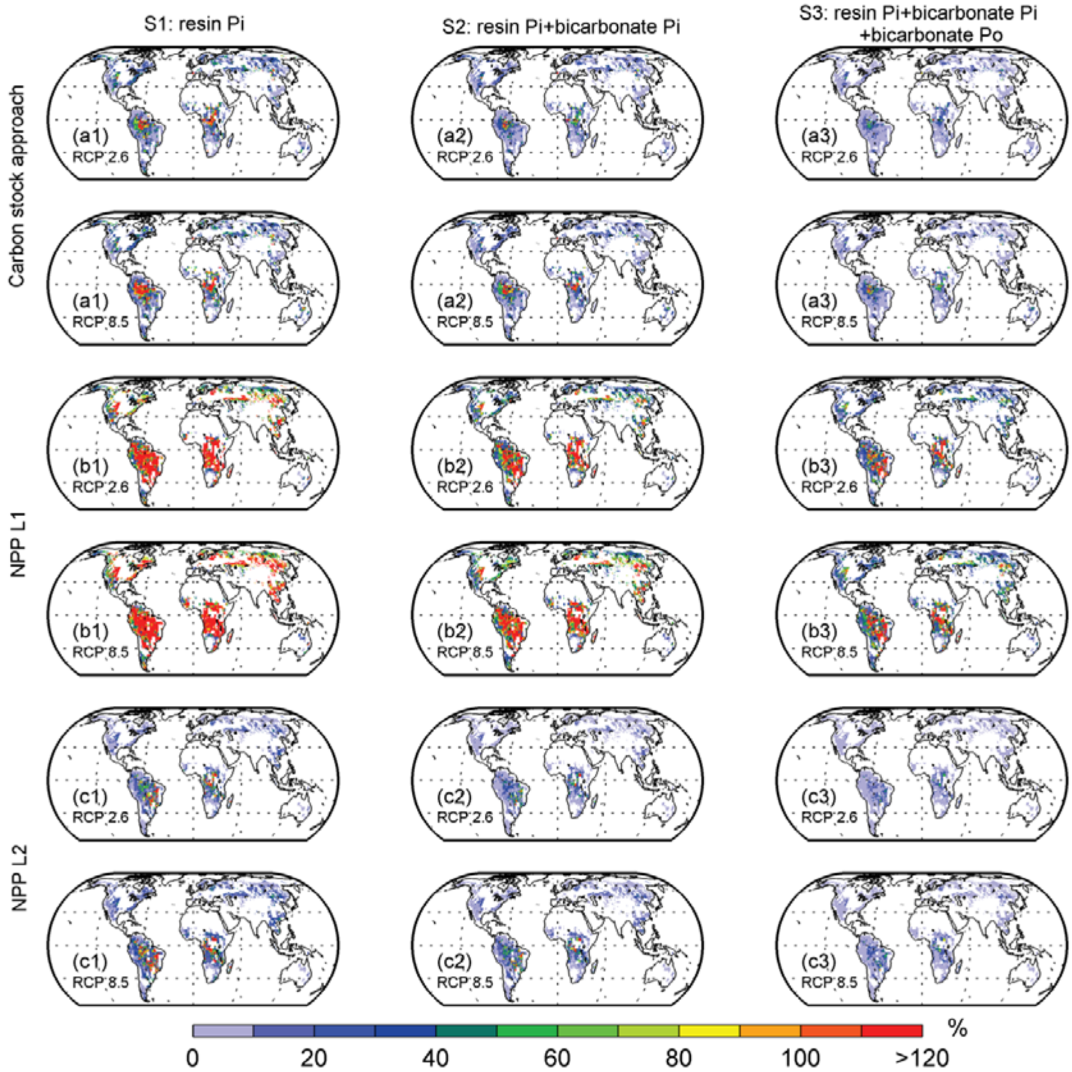

Figure S12 Utilization rate of available soil P by the year 2100 derived from the carbon stock approach (a), the NPP_L1 (b) and the NPP_L2 scenarios (c). Different assumptions for the amount of available soil P are denoted by numbers 1-3 with available P being resin Pi (1), labile Pi (2) or total labile P (3).

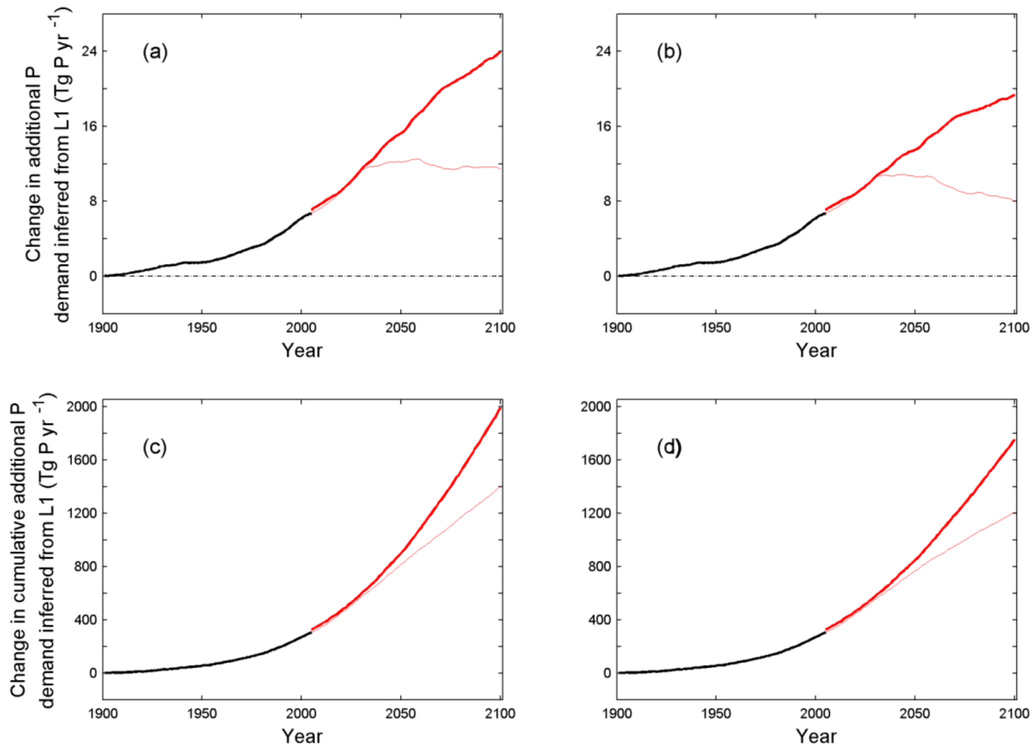

Figure S13 Changes of additional P demand (running average with 15-years window) and cumulative additional P demand by NPP_L1 approach relative to 1900-1910 derived from IPSL-CM5A-MR. (a) and (c) are derived from the constant vegetation C:P ratios by literature (Table 2). (b) and (d) are derived by assuming that C:P ratios of leaf, wood and root all increase linearly with time after 2005 (9% by 2100).

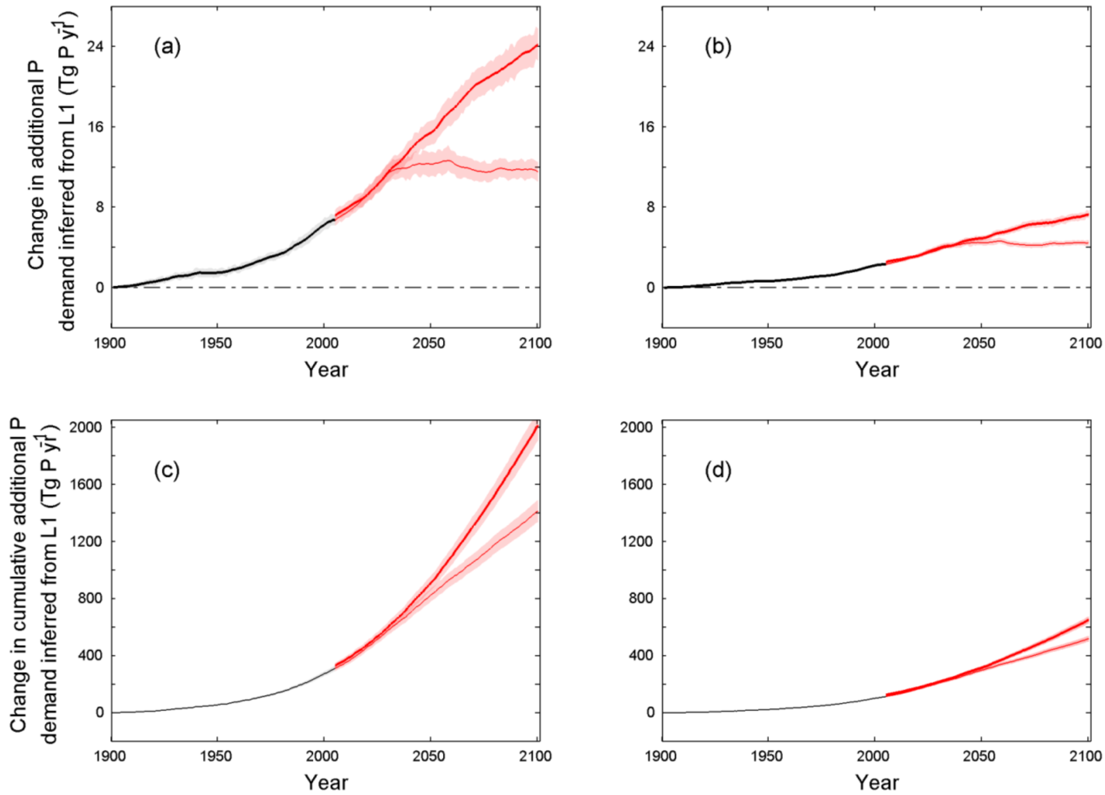

Figure S14 Changes of annual additional P demand (running average with 15-years window) and cumulative additional P demand by NPP_L1 approach relative to 1900-1910 derived from IPSL-CM5A-MR. (a) and (c) are derived from constant NPP allocations (Table 2); while (b) and (d) are derived from modeled allocations by IPSL model. Thin and thick solid lines represent simulations with RCP 2.6 and RCP 8.5, respectively. Shading indicates the variations of P demand (standard deviation) considering the uncertainty of C:P ratios of plant tissues.

Model name	Original grid size (latitude × longitude)	Ensembles per version			PFT variables				
		Historical	RCP2.6	RCP8.5	Tree	Grass	Pasture	Shrub	Crop
IPSL-CM5A-MR	2.50° × 1.3°	3	1	1	√	√			√
MIROC-ESM-CHEM	2.81° × 2.8°	1	1	1	√	√	√		√
BNU-ESM	2.81° × 2.8°	1	1	1	√	√		√	

Table S1 Basic information of three ESMs used in this study.

		C-stock approach							NPP approach					
		Global		Tropical		Extra-tropical			Global		Tropical		Extra-tropical	
		RCP 2.6	RCP 8.5	RCP 2.6	RCP 8.5	RCP 2.6	RCP 8.5		RCP 2.6	RCP 8.5	RCP 2.6	RCP 8.5	RCP 2.6	RCP 8.5
IPSL_CM5A_MR	S0	156.3±17.2	224.2±19.6	92.0±14.4	154.2±18.0	64.2±5.8	70.0±3.9	L1	960.7±81.0	1428.9±109.8	595.0±51.9	906.9±70.9	344.3±29.8	522.0±39.4
								L2	85.0±11.0	149.3±17.8	52.3±7.3	93.6±11.5	30.5±3.8	55.7±6.5
	S1	22.8±8.1	56.4±13.0	22.0±7.8	55.2+12.8	0.8±0.5	1.2±0.6	L1	557.1±71.0	895.9±100.0	423.2±48.5	697.5±67.4	93.3±22.8	198.4±33.0
								L2	12.5±3.9	24.2±6.5	9.9±3.4	23.1±5.3	0.5±0.5	1.1±1.1
	S2	10.2±4.6	33.2±10.1	10.2±4.6	33.1±10.1	0.0	0.0±0.1	L1	387.4±61.3	628.5±87.2	302.8±43.8	526.3±62.1	44.1±17.8	102.1±25.6
								L2	3.8±2.0	9.0±3.3	3.1±1.9	8.7±2.9	0.2±0.2	0.3±0.4
	S3	2.6±1.9	12.7±5.2	2.6±1.9	12.7±5.2	0.0	0.0	L1	216.9±46.9	350.8±66.6	177.1±34.9	313.0±49.6	15.2±12.4	37.8±17.4
								L2	0.7±0.5	1.5±1.0	0.8±0.5	1.5±1,0	0.0	0.1
MIROC_ESM_CHEM	S0	252.2±58.8	280.0±68.3	88.5±25.2	96.7±28.0	163.6±39.8	183.3±46.7	L1	669.0±94.5	847.7±113.1	311.8±46.8	374.5±52.0	357.2±48.1	473.2±61.5
								L2	66.0±12.5	89.5±17.2	29.7±6.1	36.3±6.9	36.2±6.4	53.1±10.2
	S1	75.4±33.9	90.7±42.1	29.4±15.3	35.4±18.2	46.0±21.8	55.2±27.7	L1	325.8±74.6	437.2±92.8	196.6±38.5	237.4±42.6	129.1±36.3	199.8±50.4
								L2	4.0±1.6	4.5±1.6	4.0±1.5	4.4±1.4	0.0	0.0
	S2	44.1±23.1	52.3±29.2	16.7±10.3	20.4±12.7	27.5±14.9	31.9±18.9	L1	200.2±55.5	274.8±71.7	136.1±31.0	168.2±35.1	64.1±24.7	106.6±36.8
								L2	1.7±0.6	2.4±0.7	1.7±0.6	2.4±0.7	0.0	0.0
	S3	23.9±13.6	27.1±16.4	8.0±5.9	10.0±7.4	15.9±9.3	17.2±10.7	L1	97.2±30.6	131.4±41.6	76.9±18.9	93.2±22.7	20.3±11.7	38.2±19.0
								L2	0.3±0.3	1.0±0.4	0.3±0.3	1.0±0.4	0.0	0.0
BNU_ESM	S0	159.0±26.3	221.6±34.5	61.7±11.1	100.1±14.8	97.3±20.6	121.6±25.9	L1	431.8±27.7	700.8±44.1	200.1±10.2	328.7±16.3	231.6±21.9	372.1±34.3
								L2	37.9±4.4	72.2±9.6	14.4±1.2	29.7±3.1	23.4±3.6	42.5±7.5
	S1	6.9±4.6	19.1±9.4	2.3±1.4	8.3±3.8	4.5±4,3	10.9±8.0	L1	82.9±11.0	207.9±27.3	61.8±5.5	136.0±11.1	21.1±8.3	71.9±21.2
								L2	0.1±0.0	1.2±0.4	0.1	1.2±0.4	0.0	0.0
	S2	1.1±1.3	5.5±4.0	0.3±0.4	2.4±1.8	0.8±1.2	3.1±3.4	L1	33.2±4.2	89.6±12.6	28.8±3.0	70.0±6.6	4.5±2.6	19.5±8.9
								L2	0.0	0.0	0.0	0.0	0.0	0.0
	S3	0.0±0.1	1.1±1.3	0.0	0.6±0.9	0.0±0.1	0.5±1.0	L1	7.3±1.4	30.0±4.0	7.0±1.3	28.0±3.2	0.3±0.4	2.1±1.8
								L2	0.0	0.0	0.0	0.0	0.0	0.0

Table S2 The total potential P deficit (mean value ± standard deviation; including the uncertainties of C:P for plant tissues) derived from C stock and NPP approach by each model and each scenario for available soil P.

		Total C stock						Vegetation						Soil					
		Global		Tropical		Extra-tropical		Global		Tropical		Extra-tropical		Global		Tropical		Extra-tropical	
		RCP 2.6	RCP 8.5	RCP 2.6	RCP 8.5	RCP 2.6	RCP 8.5	RCP 2.6	RCP 8.5	RCP 2.6	RCP 8.5	RCP 2.6	RCP 8.5	RCP 2.6	RCP 8.5	RCP 2.6	RCP 8.5	RCP 2.6	RCP 8.5
IPSL_CM5A	S_{CMIP5}	189.0	321.9	75.6	155.1	113.4	166.8	141.1	295.5	50.7	129.2	90.3	166.3	20.7	0.4	14.5	14.0	6.2	-13.6
	S0	7.8	58.3	-30.0	-30.0	37.8	88.4	17.9	101.5	-23.7	-11.0	41.6	112.5	-2.7	-26.7	0.7	-4.2	-3.5	-22.5
	S1	160.9	243.6	48.6	78.0	112.3	165.6	119.6	232.9	30.1	67.4	89.5	165.4	18.2	-5.0	12.1	8.7	6.1	-13.7
	S2	176.9	275.5	63.5	108.7	113.4	166.8	131.7	258.1	41.4	91.8	90.3	166.2	19.7	-2.6	13.5	11.0	6.2	-13.6
	S3	186.3	304.7	72.9	138.0	113.4	166.8	139.0	281.6	48.6	115.4	90.3	166.2	20.5	-0.6	14.3	13.0	6.2	-13.6
MIROC_ES	S_{CMIP5}	-49.6	-119.1	-54.1	-69.5	4.5	-49.7	-67.2	-80.1	-34.6	-38.6	-32.6	-41.4	42.6	16.6	-11.7	-21.0	54.3	37.6
	S0	-168.6	-232.4	-101.2	-115.6	-67.4	-116.8	-92.5	-100.4	-45.8	-48.4	-46.7	-52.0	-22.0	-48.7	-37.7	-47.3	15.7	-1.5
	S1	-77.5	-150.6	-66.1	-84.0	-11.4	-66.6	-71.6	-84.1	-36.6	-40.4	-35.0	-43.7	26.7	-2.5	-18.9	-30.2	45.6	27.8
	S2	-62.6	-133.3	-58.9	-75.6	-3.7	-57.7	-69.2	-81.8	-35.2	-39.2	-34.0	-42.6	35.4	8.2	-14.6	-24.9	50.0	33.0
	S3	-55.8	-125.3	-55.8	-71.9	-0.1	-53.4	-68.3	-80.8	-34.8	-38.9	-33.5	-41.9	39.4	13.1	-12.6	-22.4	52.0	35.5
BNU_ESM	S_{CMIP5}	126.4	178.5	47.7	103.0	78.7	75.6	32.5	71.2	32.4	81.6	0.2	-10.4	71.8	83.3	13.2	17.7	58.6	65.7
	S0	-19.2	-38.8	-42.8	-46.4	23.6	7.6	-77.1	-98.8	-49.9	-54.7	-27.1	-44.0	48.7	53.9	8.0	9.5	40.6	44.4
	S1	123.2	164.6	45.1	91.8	78.2	72.8	30.0	60.3	29.9	71.3	0.1	-11.0	71.4	81.5	13.0	17.1	58.4	64.4
	S2	126.2	175.4	47.5	100.5	78.7	75.0	32.3	68.8	32.1	79.3	0.1	-10.5	71.8	82.8	13.2	17.5	58.6	65.3
	S3	126.4	178.1	47.7	102.7	78.7	75.4	32.5	70.9	32.4	81.3	0.2	-10.4	71.8	83.2	13.2	17.6	58.6	65.5

Table S3 Changes in C stock (Pg C) in 2090s compared to 1900s by CMIP5 simulations (S_{CMIP5}, marked as red in the table) and changes of reconstructed C stock due to P limitation based on the four scenarios of available soil phosphorus (S0-S3) in the three ESMs.

			Global		Tropical		Extra-tropical	
			RCP 2.6	RCP 8.5	RCP 2.6	RCP 8.5	RCP 2.6	RCP 8.5
IPSL_CM5A_MR	S_{CMIP5}		19.3	41.4	11.5	22.1	7.8	19.3
	S0	L1	1.9	5.2	1.1	2.7	0.8	2.5
		L2	3.8	15.0	2.2	7.9	1.6	7.1
	S1	L1	8.8	20.3	3.2	6.2	5.6	14.1
		L2	16.8	37.3	9.1	18.2	7.7	19.1
	S2	L1	11.1	24.3	4.5	7.8	6.6	16.5
		L2	18.5	37.9	10.7	18.7	7.8	19.2
	S3	L1	14.3	30.6	7.1	12.6	7.2	18.0
		L2	19.1	41.2	11.3	21.9	7.8	19.3
MIROC_ESM_CHEM	S_{CMIP5}		7.4	15.0	1.7	3.9	5.7	11.2
	S0	L1	-2.9	-3.2	-2.2	-2.9	-0.7	-0.3
		L2	-2.3	1.2	-1.9	-0.7	-0.4	1.8
	S1	L1	2.5	6.5	-1.1	-0.2	3.6	6.7
		L2	6.9	14.5	1.2	3.3	5.7	11.2
	S2	L1	4.0	9.2	-0.5	0.8	4.5	8.4
		L2	7.2	14.7	1.5	3.5	5.7	11.2
	S3	L1	5.6	12.2	0.4	2.0	5.2	10.1
		L2	7.3	14.8	1.6	3.6	5.7	11.2
BNU_ESM	S_{CMIP5}		12.0	27.4	4.7	11.4	7.3	16.0
	S0	L1	0.5	-0.5	0.2	-0.5	0.3	0.1
		L2	2.0	8.3	1.1	4.0	0.9	4.3
	S1	L1	9.6	17.9	3.0	5.6	6.6	12.3
		L2	12.0	27.2	4.7	11.2	7.3	16.0
	S2	L1	11.1	22.9	3.9	8.1	7.2	14.8
		L2	12.0	27.3	4.7	11.4	7.3	16.0
	S3	L1	11.7	25.6	4.3	9.7	7.3	15.8
		L2	12.0	27.4	4.7	11.4	7.3	16.0

Table S4 Changes in NPP (Pg C yr^{-1}) in 2090s compared to 1900s by CMIP5 simulations (S_{CMIP5}, marked as red) and changes in reconstructed NPP due to P limitation based on the four scenarios of available soil phosphorus (S0-S3) and the two scenarios of litter decomposition (L1 and L2) in the three ESMs.

	RCP2.6		RCP8.5	
	Additional P demand derived from constant C:P ratios	Additional P demand derived from flexible C:P ratios	Additional P demand derived from constant C:P ratios	Additional P demand derived from flexible C:P ratios
2000s	56.1	55.5 (0.5%)	56.6	56.0 (0.5%)
2040s	106.1	89.0 (4.2%)	137.8	119.8 (4.2%)
2090s	131.5	93.8 (9%)	223.0	176.5 (9%)

Table S5 Additional P demand (Tg) derived from IPSL_CM5A_MR by the C stock-based approach by using constant vegetation C:P ratios and flexible vegetation C:P ratios. It is assumed that C:P ratios of leaf, wood and root all increase linearly with time after 2005 (9% by 2100). Numbers in parentheses indicate the rate of increase for flexible vegetation during different periods.